

SINGLE-SIDED MAGNETIC NANOPARTICLES IMAGING SCANNER FOR  
EARLY DETECTION OF BREAST CANCER

ABDULKADIR ABUBAKAR SADIQ

A thesis submitted in  
fulfillment of the requirement for the award of the  
Doctor of Philosophy of Electrical Engineering



Faculty of Electrical and Electronics Engineering  
Universiti Tun Hussein Onn Malaysia

SEPTEMBER 2018

Dedicated to my late parents Alhaji Abdulkadir Adamu and Hajiya Zainab

Abdulkadir



## ACKNOWLEDGEMENT

All thanks and gratitude are undoubtedly due to Allah the most exalted for all His favours.

Firstly, I would like to express my sincere gratitude to my supervisor Associate Professor Dr Muhammad Mahadi Abdul Jamil for the continuous support of my PhD study and related research, for his patience, motivation, and immense knowledge. His guidance helped me in all the time of research and writing of this thesis. I also owe special thanks to my Co-supervisor in the person of Dr Nurmiza Binti Othman. Her guidance and unending inspiration were equally instrumental towards the success of my research.

This research is funded by the Ministry of Higher Education Malaysia under Research Acculturation Grant Scheme (RAGS) Vot No. R067, Short Term Grant Vot No. U117 and Postgraduate Research Grant (GPPS) Vot No. U589, Universiti Tun Hussein Onn Malaysia (UTHM). Therefore, I would like to thank the Office for Research, Innovation, Commercialization and Consultancy Management (ORICC), Universiti Tun Hussein Onn Malaysia for providing me with these research grants without which this research would have been challenging. I thank my fellow lab mates for the stimulating discussions, for the sleepless nights we were working together before deadlines, and for all the fun we have had in the last three years.

Last but not the least, I would like to thank my brothers, sisters and friends for supporting me spiritually throughout the PhD journey and my life in general, I appreciate your strong faith in me. Special thanks to my wife Samira Sani for her patience, constant encouragement, love, sacrifice and special prayers, and to my children Mahir and Muhib for their love and patience.

May Allah rewards everyone in the best of ways.

## ABSTRACT

Electromagnetic coils form the basis of magnetic particle imaging (MPI) scanners. Previous scanner designs employ Helmholtz coil arrangement which has low sensitivity and high cost of fabrication. Furthermore, the scanners have long signal acquisition time and high memory requirement. This research focuses on developing a simple, low-cost and low memory demanding one-dimensional MPI scanner capable of imaging the position and concentration of magnetic nanoparticles (MNPs), using electromagnetic coils in the form of solenoids. The scanner produces an oscillatory magnetic field to excite the MNPs and a static magnetic field to confine the region of interest. The MNPs reacted with a nonlinear magnetisation response, inducing a voltage signal that was measured with an appropriate gradiometer pickup coil. In Fourier space, the received voltage signal consists of the fundamental excitation frequency and harmonics. This research utilises the second harmonic response of the MNPs to determine their position and concentration. Analogue Bandpass and Bandstop filters were designed for signal excitation and reception. Resovist and Perimag MNPs in liquid and immobilised form were used as tracer materials, which were moved to different spatial positions through the field of view (FOV), to record the induced voltages. The magnitude response of the Bandpass filter with 22.8 kHz fundamental frequency shows a flat amplitude in the passband with a smooth roll-off rate of  $\pm 80$  dB/pole, while the Bandstop filter efficiently attenuates the fundamental frequency and passed the 45.6 kHz second harmonic frequency. Results of the excitation coil design revealed that a magnetic field within the range of 0.8 mT to 4.4 mT was obtained, while a voltage in microvolts range was induced in the gradiometer pickup coil. The contour maps derived from imaging one and two samples of the MNPs in the *XY*-plane revealed their position and shape. Additionally, the average threshold of the peak signal amplitude was obtained as 10.63  $\mu$ V that would indicate the presence of MNPs concentration sufficient for cancer detection. The developed single-sided MPI scanner has a spatial resolution of less than 1 mm, a pixel resolution of 51.5 megapixels and 42.1 ms image acquisition time. Thus, the outcome of this research showed that the developed single-side MPI scanner has a potential in the detection of MNPs, which could help in sentinel lymph node biopsy for breast cancer diagnosis.

## ABSTRAK

Gegelung elektromagnet membentuk asas pengimbas zarah magnet (MPI). Rekaan pengimbas sebelumnya menggunakan pengaturan gegelung Helmholtz yang mempunyai kepekaan yang rendah dan kos fabrikasi yang tinggi. Selain itu, pengimbas mempunyai masa ambilan isyarat yang lama dan memerlukan *memory* yang tinggi. Kajian ini tertumpu kepada pembangunan pengimbas MPI yang ringkas, berkadar rendah dan penggunaan *memory* yang rendah dalam satu dimensi yang mampu mengimbas kedudukan dan kepekatan nanopartikel magnetik (MNPs), dengan menggunakan gegelung elektromagnet dalam bentuk solenoid. Pengimbas menghasilkan medan magnet *oscillatory* bagi mengalakkan MNPs dan medan magnet statik untuk menghadkan kawasan tertumpu. MNP memberi tindak balas kepada *nonlinear magnetisation*, dan menghasilkan isyarat voltan yang diukur dengan gegelung pikap *gradiometer* yang bersesuaian. Di dalam ruang Fourier, isyarat voltan yang diterima terdiri daripada asas frekuensi pengujaan dan harmonik. Kajian ini menggunakan tindak balas harmonik kedua MNP untuk menentukan kedudukan dan kepekatan MNP. Penapisan *Bandpass* dan *Bandstop* Analog telah direka bagi pengujaan dan penerimaan isyarat. MNP *Resovist* dan *Perimag* dalam bentuk cecair dan *immobilized* telah digunakan sebagai bahan pengesan, yang dialihkan ke kedudukan spasial yang berlainan melalui bidang pandangan atau dikenali sebagai *Field of View* (FOV), bagi mencatat voltan teraruh. Tindak balas magnitud penapis *Bandpass* dengan frekuensi asas 22.8 kHz menunjukkan amplitud rata di passband dengan kadar *roll-off* pada  $\pm 80$  dB / pole, manakala penapis *Bandstop* cekap mengatasi frekuensi asas dengan 45.6 kHz dan melepasi frekuensi harmonik kedua. Keputusan menunjukkan reka bentuk pengujaan gegelung medan magnet didalam julat antara 0.8 mT hingga 4.4 mT telah diperolehi, manakala pelbagai nilai voltan dalam mikrovolt diinduksi ke dalam gegelung pikap *gradiometer*. Peta kontur yang diperolehi daripada pengimejan satu dan dua sampel MNP dalam *XY-plane* menunjukkan kedudukan dan bentuknya. Di samping itu, maksima purata isyarat puncak amplitud diperolehi adalah 10.63  $\mu$ V yang akan menunjukkan kehadiran

kepekatan MNP yang memadai untuk mengesan sel kanser. Pengimbas MPI satu dimensi yang dimajukan mempunyai resolusi spatial kurang dari 1 mm, resolusi piksel 51.5 megapixel dan masa pemerolehan imej 42.1 ms. Oleh itu, hasil kajian ini menunjukkan bahawa pengimbas MPI satu dimensi yang dimajukan mempunyai potensi untuk mengesan MNPs, yang boleh membantu dalam biopsi nodus limfa sentinen untuk diagnosis kanser payudara.



PTTHM  
PERPUSTAKAAN TUNKU TUN AMINAH

## CONTENTS

<b>TITLE</b>	<b>i</b>
<b>DECLARATION</b>	<b>ii</b>
<b>DEDICATION</b>	<b>iii</b>
<b>ACKNOWLEDGEMENT</b>	<b>ii</b>
<b>ABSTRACT</b>	<b>iii</b>
<b>ABSTRAK</b>	<b>iv</b>
<b>CONTENTS</b>	<b>vi</b>
<b>LIST OF TABLES</b>	<b>x</b>
<b>LIST OF FIGURES</b>	<b>xi</b>
<b>LIST OF SYMBOLS AND ABBREVIATIONS</b>	<b>xv</b>
<b>LIST OF APPENDICES</b>	<b>xx</b>
<b>CHAPTER 1 INTRODUCTION</b>	<b>1</b>
1.1 Research background	1
1.2 Problem statement	4
1.3 Aim and objectives	5
1.4 Scope of the research	6
1.5 Thesis outline	6
1.6 Contributions of the research	7
<b>CHAPTER 2 LITERATURE REVIEW</b>	<b>9</b>
2.1 Introduction	9
2.2 Medical imaging methods	10
2.3 Magnetic particle imaging method	12
2.3.1 Alignment of MNPs with oscillating magnetic field	12
2.3.2 Creation of field free region (FFR)	13
2.3.3 MPI signal induction	15
2.4 MPI scanner geometries	16
2.5 Applications of MPI	18

2.5.1	Cancer detection and treatment	18
2.5.2	Diagnosis of cardiovascular diseases (CVD)	20
2.5.3	Lungs and stomach imaging	20
2.5.4	Cell tracking and labelling	21
2.6	Magnetic nanoparticles in MPI	21
2.6.1	Synthesis of MNPs	22
2.6.2	Advantages of MNPs	24
2.7	Detection methods of MNPs	25
2.8	Biomedical applications of magnetic nanoparticles	27
2.8.1	Imaging	27
2.8.2	Drug delivery	27
2.8.3	Immunoassay	28
2.8.4	Hyperthermia	28
2.9	MPI image reconstruction	29
2.9.1	Projection-based reconstruction (PBR)	30
2.9.2	System matrix-based reconstruction	30
2.9.3	Time-based system matrix	30
2.9.4	Frequency space system matrix	31
2.9.5	Measurement-based system matrix	32
2.9.6	Model-based system matrix	33
2.9.7	Hybrid system matrix	34
2.9.8	Computing MNPs concentration	35
2.10	Single-sided MPI scanner topology	37
2.11	Summary	38
<b>CHAPTER 3 MATERIALS AND METHODS</b>		<b>40</b>
3.1	Introduction	40
3.2	Single-sided MPI scanner	41
3.2.1	Fundamental principle	41
3.2.2	Proposed single-sided MPI scanner	43
3.2.3	Signal chain of single-sided MPI scanner	45
3.3	Single-sided MPI scanner realisation	46
3.3.1	Electromagnetic coils for single-sided MPI scanner	46



3.3.2 Analogue filters design for single-sided MPI scanner	47
3.3.3 Resonant circuit	64
3.3.4 Other equipment used	66
3.4 Magnetic material	69
3.4.1 MNPs sample preparation	71
3.5 Software used	71
3.6 Image reconstruction	71
3.6.1 Kaczmarz method	72
3.7 Statistical analysis	73
3.8 Summary	74
<b>CHAPTER 4 ELECTROMAGNETIC COILS DESIGN FOR SINGLE-SIDED MAGNETIC PARTICLE IMAGING</b>	<b>76</b>
4.1 Introduction	76
4.2 Excitation coil design	77
4.2.1 Design procedure	78
4.2.2 Magnetic field generation	78
4.2.3 Magnetic field a solenoid	79
4.2.4 MATLAB excitation coil simulation	81
4.2.5 ANSYS Maxwell excitation coil simulation	83
4.3 Selection field coil design	87
4.4 Receive coil (pickup coil) design	90
4.4.1 Principle of gradiometer pickup coil	91
4.4.2 Surface area of pickup coil	94
4.4.3 Methodology	95
4.4.4 Voltage induced in pickup coil	96
4.4.5 Results and discussion	97
4.5 Summary	103
<b>CHAPTER 5 SECOND HARMONIC SIGNAL DETECTION OF MNPs</b>	<b>105</b>
5.1 Introduction	105
5.2 Second harmonic detection of MNPs	105
5.3 Materials and methods	106
5.3.1 Scanner set-up	106
5.3.2 MNPs preparation	108

5.4	Experiments performed	110
5.4.1	System matrix simulation	111
5.5	Results and Discussion	114
5.5.1	Sensitivity of the developed scanner	114
5.5.2	Second harmonic signal measurements	115
5.6	MNPs position estimation	119
5.6.1	Detection of one sample Resovist MNPs	119
5.6.2	Detection of one sample Perimag MNPs	124
5.6.3	Detection of two samples	127
5.6.4	Threshold for cancer detection	132
5.6.5	Image resolution	133
5.7	Summary	134
<b>CHAPTER 6 CONCLUSION AND RECOMMENDATIONS</b>		<b>136</b>
6.1	Conclusion	136
6.2	Recommendations	138
<b>REFERENCES</b>		<b>139</b>
<b>APPENDICES</b>		<b>155</b>
<b>LIST OF PUBLICATIONS</b>		<b>167</b>
<b>VITA</b>		<b>171</b>



## LIST OF TABLES

2.1	Comparison of established medical imaging modalities	11
2.2	Overview of MPI scanners	18
2.3	Overview of types of tracers used in MPI	24
2.4	Summary of previous single-sided MPI scanner designs	38
3.1	Electromagnetic coils specifications	47
3.2	Overview of BPF RC components	53
3.3	MATLAB BPF specifications	55
3.4	Summary of BSF RC components	60
3.5	MATLAB BSF parameters	62
3.6	MNPs sample specifications	70
4.1	Excitation coil specifications	87
4.2	SFC specification	90
4.3	Gradiometer pickup coil specifications	97
5.1	Single-sided MPI scanner coils parameters	108
5.2	96-well cell culture plate dimensions	108
5.3	Resovist and Perimag MNPs parameters	109
5.4	Linear regression parameters for one liquid Resovist sample	121
5.5	Linear regression parameters for one immobilised Resovist sample	123
5.6	Linear regression parameters for one liquid Perimag sample	125
5.7	Linear regression parameters for one immobilised Perimag sample	127
5.8	Linear regression parameters for two liquid Resovist samples	130
5.9	Linear regression parameters for two immobilised Perimag samples	132
5.10	Peak signal amplitude threshold for cancer detection	133

## LIST OF FIGURES

1.1	Particle Magnetisation	2
2.1	Research Fundamental Areas	10
2.2	Magnetic Nanoparticles Saturation in an Oscillating Magnetic Field	12
2.3	Field Free Point Formation	14
2.4	Field Free Line Creation	14
2.5	MPI Scanner Topologies	17
2.6	Sentinel Lymph Node	19
2.7	Schematic Diagram of Spherical and Dextran-coated MNP	22
2.8	Simulation steps of system matrix modelling	34
3.1	Single-sided Scanner Coils Arrangement	42
3.2	Proposed MPI Scanner	44
3.3	Realised Single-sided MPI Scanner	45
3.4	Ideal BPF Filter Magnitude Response	51
3.5	Unity Gain Conventional Two-Pole Active Filter	51
3.6	NI Multisim Circuit Implementation for Fourth-Order Butterworth Active BPF	54
3.7	BPF Gain Response Frequency Specifications using MATLAB	54
3.8	MATLAB BPF Magnitude Response Simulation Result	56
3.9	BPF magnitude response for NI Multisim simulation and experiment	56
3.10	Ideal characteristics of BSF	58
3.11	Principle of operation of BSF	59
3.12	BSF Schematics	61
3.13	NI Multisim Implementation of BSF	62
3.14	Magnitude response of BSF MATLAB Simulation	63
3.15	BSF NI Multisim Simulation and Experimental Results	64
3.16	Resonant Circuit for Second Harmonic Detection	65

3.17	BK 4055 Function Generator	67
3.18	HP 8447F H64 Power Amplifier	68
3.19	Tektronix PS280 Power Supply	68
3.20	NI USB-6009 DAQ Device	69
4.1	Solenoid	79
4.2	Magnetic field produced with varying number of turns	82
4.3	Magnetic field produced by varying Current	83
4.4	Excitation Coil in Ansys Maxwell	84
4.5	Magnetic Field plot along XZ plane	84
4.6	Magnetic Field plot along XY plane	85
4.7	Magnetic Field plot along YZ plane	86
4.8	MATLAB Simulation of SFC	88
4.9	SFC Simulation and Experimental Magnetic Field	89
4.10	Gradiometer coil schematic	91
4.11	Gradiometer arrangement a) Vertical b) Planer c) Asymmetric	92
4.12	Order of Gradiometer a) First-order b) Second-order c) Third-order	92
4.13	Gradiometer Pickup Coil Response	93
4.14	Pickup Coil Representation	94
4.15	MPI Signal Generation	95
4.16	Constructed Gradiometer Coil	96
4.17	Induced voltage with varying (a) Magnetic field and (b) Harmonic frequencies	98
4.18	Induced Voltage against (a) Amplitude of Excitation and (b) Number of Turns of Pickup Coil	99
4.19	Experimental set-up	100
4.20	Induced voltage from excitation and selection fields.	101
4.21	Induced voltage with varying distance	102
4.22	Induced voltage with fixed excitation frequency	103
5.1	Measurement System Set-up	107
5.2	Immobilised MNPs samples (a) One sample Perimag and (b) Two sample Resovist particles	110
5.3	MATLAB/Simulink System Matrix Simulation	112

5.4	Magnetisation of Resovist and Perimag in Solid and Liquid form	113
5.5	Induced voltage with varying distance along z-direction	114
5.6	Second harmonic signal dependence on different DC magnetic field for Resovist sample	115
5.7	Second harmonic signal dependence on different DC magnetic field for Perimag sample	116
5.8	Dependence of excitation magnetic field on the induced signal for Resovist	117
5.9	Dependence of second harmonic signal amplitude on AC excitation magnetic field for Perimag	118
5.10	Relationship between $H_{dc}$ and $H_{ac}$ at peak signal amplitude	119
5.11	Contour maps of one liquid Resovist sample located at (a) $z=10$ mm (b) $z=20$ mm (c) $z=25$ mm and (d) 30 mm below the pickup coil	120
5.12	Measured contour plots from one immobilised Resovist sample located at (a) $z=10$ mm (b) $z=20$ mm (c) $z=25$ mm and (d) $z=30$ mm	122
5.13	Measured contour maps of one liquid Perimag sample located at (a) $z=10$ mm (b) $z=20$ mm (c) $z=25$ mm and (d) $z=30$ mm below the pickup coil	124
5.14	Measured contour maps of one immobilised Perimag sample located at (a) $z=10$ mm (b) $z=20$ mm (c) $z=25$ mm and (d) $z=30$ mm beneath the pickup coil.	126
5.15	Measured contour plots from two Resovist samples of (a) similar weight ( $100 \mu\text{g}$ Fe each) at $z=10$ mm (b) similar weight ( $100 \mu\text{g}$ Fe each) at $z=20$ mm (c) different weight ( $50 \mu\text{g}$ Fe and $100 \mu\text{g}$ Fe) at $z=10$ mm and (d) different weight ( $50 \mu\text{g}$ Fe and $100 \mu\text{g}$ Fe) at $z=20$ mm beneath the pickup coil and were separated by 10 mm (centre-to-centre).	129
5.16.	Contour plots from two Perimag samples of (a) similar weight ( $100 \mu\text{g}$ Fe each) at $z=10$ mm (b) similar weight ( $100 \mu\text{g}$ Fe each) at $z=20$ mm (c) different weight ( $50 \mu\text{g}$ Fe and $100 \mu\text{g}$ Fe)	

at  $z=10$  mm and (d) different weight ( $50 \mu\text{g Fe}$  and  $100 \mu\text{g Fe}$ ) at  $z=20$  mm under the pickup coil and were separated by 10 mm (centre-to-centre).



## LIST OF SYMBOLS AND ABBREVIATIONS

$A_D$	-	Drive field amplitude
$B_S$	-	Magnetic flux density
$F_e$	-	Ferrum
$H_0$	-	Amplitude of excitation frequency
$H_D$	-	Drive magnetic field
$H_S$	-	Selection magnetic field
$H_{ac}$	-	Alternating current magnetic field
$H_{dc}$	-	Direct current magnetic field
$M_S$	-	Saturation magnetisation
$T_m$	-	Total acquisition time
$V_0$	-	Known volume
$V_h$	-	Hydrodynamic volume
$V_m$	-	Magnetic core volume
$V_{pp}$	-	Voltage peak-to-peak
$X_C$	-	Capacitive reactance
$X_L$	-	Inductive reactance
$c_{0,c}$	-	Nanoparticles concentration
$f_0$	-	Fundamental frequency
$f_D$	-	Drive field frequency
$f_c$	-	Centre frequency
$f_r$	-	Resonant frequency
$f_s$	-	Selection field frequency
$k_B$	-	Boltzmann constant
$m_s$	-	Magnetic moment at saturation
$\bar{\mu}$	-	Mean magnetic moment
$\mu_0$	-	Permeability of vacuum



$\tau_0$	-	Time constant
$\tau_B$	-	Brownian relaxation
$\tau_N$	-	Neel relaxation
$\tau_{eff}$	-	Effective relaxation
$^{\circ}C$	-	Degree Celsius
$h$	-	Sensitivity profile of magnetic field
$A$	-	Amperes
$A/m$	-	Ampere per meter
$BW$	-	Bandwidth
$C$	-	Capacitance
$D$	-	Nanoparticle diameter
$G$	-	Gradient matrix
$GHz$	-	Giga hertz
$H$	-	Magnetic field strength
$I$	-	Current
$K$	-	Anisotropy energy
$L$	-	Inductance
$M$	-	Magnetisation
$N$	-	Number of turns
$P$	-	Coil sensitivity
$Q$	-	Quality factor
$R$	-	Resistance
$RC$	-	Resistance-capacitance
$S$	-	System Matrix
$T$	-	Absolute temperature
$V$	-	Voltage
$W$	-	Weighting matrix
$X$	-	Reactance
$Z$	-	Impedance
$dB$	-	Decibel
$k\Omega$	-	Kilo ohms
$kHz$	-	Kilo hertz
$mV$	-	Millivolt

$mg$	-	Milligram
$r$	-	Spatial point
$t$	-	Time
$u$	-	Recorded signal
$\zeta$	-	Damping factor
$\eta$	-	Dynamic viscosity
$\lambda$	-	Regularization parameter
$\mu l$	-	Microliter
$\xi$	-	Langevin parameter
$\omega$	-	Angular frequency
1D	-	One-dimensional
2D	-	Two-dimensional
3D	-	Three-dimensional
AC	-	Alternating current
ACS	-	Alternating current susceptibility
ART	-	Algebraic reconstruction technique
AWG	-	American wire gauge
BPF	-	Bandpass filter
BSF	-	Bandstop filter
CAD	-	Computer-aided design
CAD	-	Coronary artery disease
CT	-	Computed tomography
DAC	-	Digital-to-analogue converter
DAQ	-	Data acquisition
DC	-	Direct current
DDS	-	Direct digital synthesis
DNA	-	Deoxyribonucleic acid
EC	-	Excitation coil
FC-PC	-	field cancellation pickup coil
FFL	-	Field free line
FFP	-	Field free point
FFR	-	field free region
FOV	-	Field of view

GB	- Gigabyte
HDD	- Hard drive
HPF	- Highpass filter
IDC	- Inductive ductal carcinoma
LabVIEW	- Laboratory virtual instrument engineering workbench
LPF	- Lowpass filter
MATLAB	- Matrix laboratory
MNPs	- Magnetic nanoparticles
MPI	- Magnetic particle imaging
MPS	- Magnetic particle spectrometer
MRA	- Magnetic resonance angiography
MRI	- Magnetic resonance imaging
MRX	- Magnetic relaxation
NI	- National instruments
PBR	- Projection-based reconstruction
PC	- Personal computer
PET	- Positron emission tomography
PLA	- Polylactic acid
RAM	- Random access memory
RBCs	- Red blood cells
RF	- Radio frequency
RFID	- Radio frequency identification
RLC	- Resistor-inductor-capacitor
rms	- Root mean square
RNA	- Ribonucleic acid
SFC	- Selection field coil
SLN	- Sentinel lymph node
SLNB	- Sentinel lymph node biopsy
SNR	- Signal-to-noise ratio
SPECT	- Single photon emission computed tomography
SPIO	- Superparamagnetic iron-oxide
SPIONs	- Superparamagnetic iron-oxide nanoparticles
SQUID	- Superconducting quantum interference device

SVD	- Singular value decomposition
TB	- Terabyte
THD	- Total harmonic distortion
USB	- Universal serial bus
VHF	- Very high frequency
VLf	- Very low frequency
w/w	- Weight per weight



PT TA UTHM  
PERPUSTAKAAN TUNKU TUN AMINAH

**LIST OF APPENDICES**

<b>APPENDIX</b>	<b>TITLE</b>	<b>PAGE</b>
A	Electromagnetic coils bobbin design using solidworks software	155
B	Data logging set-up in LabVIEW	156
C	Pseudo code for Kaczmarz algorithm	157
D	Publications	160



PTTA UTHM  
PERPUSTAKAAN TUNKU TUN AMINAH

## CHAPTER 1

### INTRODUCTION

#### 1.1 Research background

Magnetic particle imaging (MPI) is an innovative imaging modality that carries out a direct measurement of the magnetisation of ferromagnetic nanoparticles to quantify their local concentration. Superparamagnetic iron-oxide nanoparticles (SPIONs) are usually employed as tracer substance in MPI, due to their tiny size and exhibition of superparamagnetism. These SPIONs are injected into a target area, then excited by an external magnetic field (drive field) and the response of the particles is recorded, which is proportional to the concentration of the SPIONs (Gleich 2013, Saritas *et al.*, 2013 & Sadiq *et al.*, 2015).

MPI technique was invented in 2001 by Bernhard Gleich and Jürgen Weizenecker, who first reported about the concept in 2005. MPI offers a unique combination of features that sets it apart from other conventional methods for medical imaging. An essential theory for describing the magnetic behaviour of superparamagnetic particles is the Langevin theory, which is evident from the assumption that the particles are always in thermal equilibrium (Gleich & Weizenecker, 2005).

The spatial distribution of magnetic nanoparticles (MNPs) used as tracer material can be determined by measuring the change in magnetisation of the tracer material in a time-varying magnetic field. Figure 1.1 demonstrates the particle magnetisation, showing the relationship between the external magnetic field applied

to the MNPs and their magnetisation response. The nonlinearity of the MNPs response is depicted by the green curve in Figure 1.1.  $M$  is the magnetisation of the magnetic nanoparticles while  $H$  is the applied excitation magnetic field with peak-to-peak amplitude of  $A$  to  $-A$ .

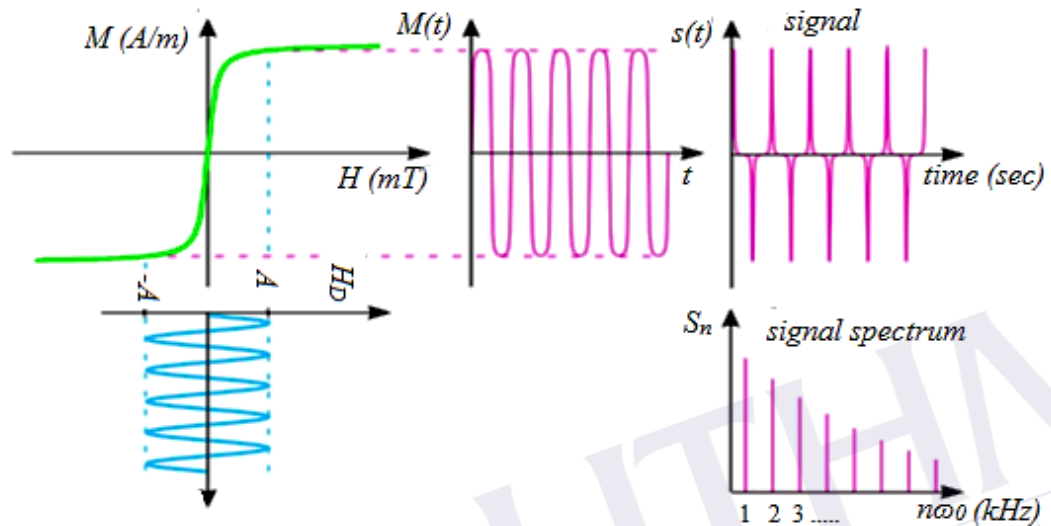


Figure 1.1: Particle Magnetisation (Borget *et al.*, 2012)

The dynamic region of the magnetisation curve is nonlinear when a periodic signal of  $-A$  to  $A$  is applied, while the saturation region started when the area used is above  $A$ . No further magnetisation is produced at saturation, and this results in the presence of harmonics in the established signal. The magnetization response  $M(t)$  with respect to time is shown next in Figure 1.1, while the corresponding voltage signal  $s(t)$  in time domain is shown after that. The harmonics from the magnetisation of the particles are obtained by conducting a fast fourier transform on  $s(t)$  to reveal the harmonic spectrum,  $S_n$  as shown in the last plot of Figure 1.1. The amplitude of the voltage signals recorded at these harmonics are used to reconstruct tomographic images that will indicate the existence of the magnetic tracer material. To spatially and temporally decide a spreading of SPIONs tracer within a patient, the communication between static and dynamic magnetic fields and the typical magnetisation behaviour of the tracer material is exploited.

The dynamic magnetic field (also known as the excitation field) is generated by an excitation coil with an AC signal source. The static magnetic field on the other hand is generated by a gradient coil (selection field coil) with a DC signal source. The

excitation magnetic field is superimposed on the selection magnetic field to create the field-free region, where only the magnetic nanoparticles contribute to the recorded signal.

MPI offers some advantages over other medical imaging methods, which could make it a suitable technique for clinical examinations (Knopp & Buzug 2012, Gräfe *et al.*, 2012). The first advantage of MPI is the quantitative measurement. The measured MPI signal is directly proportional to the concentration of the tracer material (follows a system of linear equations). That is, the higher the concentration, the stronger the signal received and vice versa. This means that no signal will be recorded when there is no tracer material present in the target area. The concentration to signal correlation is known to exist from other methods in nuclear medicine, such as the single photon emission computed tomography (SPECT), magnetic resonance imaging (MRI) and positron emission tomography (PET).

Secondly, MPI offers high spatial and temporal resolution. This advantage can further be utilised to implement a real-time MNPs imaging. The third advantage of MPI is high sensitivity in imaging. The MPI signal is acquired directly from the tracer, not from the tissues. This feature makes the sensitivity of MPI much superior to that of MRI. Additionally, MPI offers flexibility in the selection of acquisition parameters, to achieve a particular sensitivity or resolution.

Fourthly, there is no ionisation radiation in MPI. The magnetic fields used in MPI are either periodic or static, which pose no risk to patients (no adverse or long-term effects). Finally, MPI signals were reported to be acquired in less than 0.1 seconds as compared to other imaging modalities that have acquisition time of over one minute.

MPI as a medical imaging modality finds applications similar to that of the established modalities, for instance in diagnosis and treatment of diseases, and cell tracking and labelling. Moreover, MPI targets applications demanding fast, dynamic imaging, such as blood flow visualisation in the case of coronary artery diseases, cancer identification, for example, sentinel lymph node biopsy (SLNB) or any application where tracers are employed for diagnosis using a PET, SPECT or MRI (Gleich *et al.*, 2012). In conjunction with advances in imaging technologies such as MRI, computed tomography (CT), and fluoroscopy, MPI as a novel imaging technology, however, is promising in holding excellent imaging properties of sound spatial resolution, high signal-to-noise ratio (SNR), and high sensitivity without ionising emission (Utkur *et al.*, 2017).



## REFERENCES

- Ahlborg, M., Keathner, C., Szwargulski, P., Knopp, T. & Buzug, M. (2018). Patches in Magnetic particle imaging. *Bildverarbeitung fur die medizin*, 1(2), pp. 169-201.
- Akhter, S., Zaki Ahmad, M., Singh, A., Ahmad, I., Rahman, M., Anwar, M. & Krishen Khar, R. (2011). Cancer targeted metallic nanoparticle: targeting overview, recent advancement and toxicity concern. *Current pharmaceutical design*, 17(18), pp. 1834-1850.
- Appuhamillage, G. A., Reagan, J. C., Khorsandi, S., Davidson, J. R., Voit, W. & Smaldone, R. A. (2017). 3D printed remendable polylactic acid blends with uniform mechanical strength enabled by a dynamic Diels–Alder reaction. *Polymer Chemistry*, 8(13), pp. 2087-2092.
- Baker, B. C. (2015). Band stop filters and the Bainter topology. *Analogue applications Journal*, AAJ1Q, pp. 8-12.
- Basic Electronics Tutorials. (2017). Band Stop Filters are Reject Filters that Attenuate Signals. [online] Available at: <http://www.electronics-tutorials.ws/filter/band-stop-filter.html> [Accessed 13 Sep. 2017].
- Bauer, L. M., Situ, S. F., Griswold, M. A. & Samia, A. C. S. (2015). Magnetic particle imaging tracers: state-of-the-art and future directions. *Journal of Physical Chemistry Letters*, 6(13), pp. 2509-2517.
- Bente, K., Weber, M., Graeser, M., Sattel, T. F., Erbe, M. & Buzug, T. M. (2015). Electronic field free line rotation and relaxation deconvolution in magnetic particle imaging. *IEEE transactions on medical imaging*, 34(2), pp. 644-651.
- Biederer, S. (2012). *Magnetic particle spectrometer: Development of a spectrometer for the analysis of superparamagnetic iron oxide nanoparticles for magnetic particle imaging*. Springer-Verlag, Germany.
- Biederer, S., Knopp, T., Sattel, T. F., Lüdtke-Buzug, K., Gleich, B., Weizenecker, J. & Buzug, T. M. (2009). Magnetisation response spectroscopy of

- superparamagnetic nanoparticles for magnetic particle imaging. *Journal of Physics D: Applied Physics*, 42(20), pp. 205001-205007.
- Biswal, A. & Profile, A. (2012, October 27). *Butterworth filter and Chebyshev filter – A comparison*. Retrieved from <http://www.123mylist.com/2012/03/butterworth-filter-and-chebyshev-filter.html>
- Blasiak, B., van Veggel, F. C. & Tomanek, B. (2013). Applications of nanoparticles for MRI cancer diagnosis and therapy. *Journal of Nanomaterials*, 13(12), pp. 1-12.
- Bringout, G. & T. Buzug, T. (2015). Coil Design for Magnetic Particle Imaging: Application for a Preclinical Scanner. *IEEE Transaction on Magnetics*, 51(2), pp. 1-8.
- Bringout, G. (2016). Field Free Line Magnetic Particle Imaging (Doctoral dissertation). University of Lübeck, Lübeck, Germany.
- Butters, J. T., Butters, B. M., Naughton, P. & Puckette, M. (2016). U.S. Patent No. 9,417,257. Washington, DC: U.S. Patent and Trademark Office.
- Buzug, T. M., Bringout, G., Erbe, M., Gräfe, K., Graeser, M., Grüttner, M. & Haegele, J. (2012). Magnetic particle imaging: introduction to imaging and hardware realisation. *Zeitschrift für Medizinische Physik*, 22(4), pp. 323-334.
- Carmeliet, P., Eelen, G. & Kalucka, J. (2017). *Arteriogenesis versus angiogenesis: The ESC Textbook of Vascular Biology*. Oxford, England: Oxford University Press.
- Casson, A. J., Yates, D. C., Patel, S. & Rodriguez-Villegas, E. (2007, August). An analogue Bandpass filter realisation of the continuous wavelet transform. *In Engineering in Medicine and Biology Society, 29th Annual International Conference of the IEEE*, pp. 1850-1854
- Chomoucka, J., Drbohlavova, J., Huska, D., Adam, V., Kizek, R. & Hubalek, J. (2010). Magnetic nanoparticles and targeted drug delivery. *Pharmacological Research*, 62 (2010). pp 144-149.
- Cole, A. J., Yang, V. C. & David, A. E. (2011). Cancer theranostics: the rise of targeted magnetic nanoparticles. *Trends in biotechnology*, 29(7), pp. 323–32. doi:10.1016/j.tibtech.2011.03.001
- Croft, L. R., Goodwill, P. W., Konkle, J. J., Arami, H., Price, D. A., Li, A. X. & Conolly, S. M. (2016). Low drive field amplitude for improved image resolution in magnetic particle imaging. *Medical physics*, 43(1), pp. 424-435.

- Cullity, B. & Graham, C. (2011). *Introduction to Magnetic Materials*. Somerset: Wiley.
- Deatsch, A. E. & Evans, B. A. (2014). Heating efficiency in magnetic nanoparticle hyperthermia. *Journal of Magnetism and Magnetic Materials*, 354, pp. 163-172.
- Dieckhoff, J., Eberbeck, D., Schilling, M. & Ludwig, F. (2016). Magnetic-field dependence of Brownian and Néel relaxation times. *Journal of Applied Physics*, 119(4), pp. 0439031-0439038
- Du, Y., Lai, P. T., Leung, C. H. & Pong, P. W. T. (2013). Design of Superparamagnetic Nanoparticles for Magnetic particle imaging (MPI). *International Journal of Molecular Sciences*, 14(1), pp. 18682-18710.
- Dutz, S. & Hergt, R. (2014). Magnetic particle hyperthermia—a promising tumor therapy. *Nanotechnology*, 25(45), pp. 452001-452028.
- Eberbeck, D., Dennis, C. L., Huls, N. F., Krycka, K. L., Gruttner, C. & Westphal, F. (2013). Multicore magnetic nanoparticles for magnetic particle imaging. *IEEE Transactions on Magnetics*, 49(1), pp. 269-274.
- Electronics Hub. (2017). *Band Stop Filter Circuit Design and Applications*. [online] Available at: <http://www.electronicshub.org/band-stop-filter/> [Accessed 13 Sep. 2017].
- Enpuku, K., Tsujita, Y., Nakamura, K., Sasayama, T. & Yoshida, T. (2017). Biosensing utilizing magnetic markers and superconducting quantum interference devices. *Superconductor Science and Technology*, 30(5), pp. 1-12.
- Enpuku, K., Ueoka, Y., Sakakibara, T., Ura, M., Yoshida, T., Mizoguchi, T. & Kandori, A. (2014). Liquid-phase immunoassay utilizing binding reactions between magnetic markers and targets in the presence of a magnetic field. *Applied Physics Express*, 7(9), pp. 097001.
- Erbe, M. (2014). *Field Free Line Magnetic Particle Imaging*. Springer Science & Business Media.
- Erbe, M., Knopp, T., Sattel, T., Biederer, S. & Buzug, T. (2011). Experimental generation of an arbitrarily rotated field-free line for the use in magnetic particle imaging. *Medical Physics*, 38(9), pp. 5200-5207.
- Felicetti, L., Femminella, M., Reali, G. & Liò, P. (2016). Applications of molecular communications to medicine: A survey. *Nano Communication Networks*, 7, pp. 27-45.

- Fiorillo, F. (2010). Measurements of magnetic materials. *Metrologia*, 47, pp. S114-S142.
- Flotte, T. R. (2007). Gene therapy: the first two decades and the current state-of-the-art. *Journal of cellular physiology*, 213(2), pp. 301-305.
- Franco, S. (2015). *Design with operational amplifiers and analog integrated circuits*. New York: McGraw-Hill.
- Gallo, J., Long, N. J. & Aboagye, E. O. (2013). Magnetic nanoparticles as contrast agents in the diagnosis and treatment of cancer. *Chemical Society Reviews*, 42(19), pp. 7816-7833.
- Gleich, B. & Weizenecker, J. (2005). Tomographic imaging using the nonlinear response of magnetic particles, *Nature*, 435(70460), pp. 1214-1217.
- Gleich, B. (2013). *Principles and applications of magnetic particle imaging*. Springer Science & Business Media, Germany.
- Gleich, B. (2014). *Basic idea of Magnetic Particle Imaging*. In *Principles and Applications of Magnetic Particle Imaging*. Springer Fachmedien Wiesbaden.
- Goodwill, P. W. & Conolly, S. M. (2010). The X-space formulation of the magnetic particle imaging process: 1-D signal, resolution, bandwidth, SNR, SAR, and magneto stimulation. *IEEE transactions on medical imaging*, 29(11), pp. 1851-1859.
- Goodwill, P. W. & Connolly, S. M. (2011). "Multidimensional x-space magnetic particle imaging," *IEEE Transactions on Medical Imaging*, 30(9), pp. 1581–1590.
- Goodwill, P. W., Scott, G. C., Stang, P. P. & Conolly, S. M. (2009). Narrowband magnetic particle imaging. *IEEE Transactions on Medical Imaging*, 28(8), pp. 1231-1237.
- Goodwill, P. W., Konkle, J. J., Zheng, B., Saritas, E. U. & Conolly, S. M. (2012). Projection X-space Magnetic Particle Imaging. *IEEE Transactions on Medical Imaging*, 31, pp. 1076–1085.
- Graeser, M., Knopp, T., Grüttner, M., Sattel, T. & Buzug, T. (2013). Analog receive signal processing for magnetic particle imaging. *Medical Physics*, 40(4), pp. 042303.
- Gräfe, K., Sattel, T. F., Lüdtke-Buzug, K., Finas, D., Borgert, J. & Buzug, T. M. (2012). Magnetic-particle-imaging for sentinel lymph node biopsy in breast cancer. In *Magnetic Particle Imaging*. Springer, Berlin, Heidelberg.

- Gräfe, K., von Gladiss, A., Bringout, G., Ahlborg, M. & Buzug, T. M. (2015, March). 2D imaging with a single-sided MPI device. *5th International Workshop on Magnetic Particle Imaging (IWMPI)*, pp. 1-1.
- Gräfe, K., Weber, M., Sattel, T. & Buzug, T. (2013). Precision of an MPI Scanner Construction: Registration of Measured and Simulated Magnetic Fields. *Biomedical Engineering/Biomedizinische Technik*, 58(1), pp. 1-2.
- Grüttner, M., Gräser, M., Biederer, S., Sattel, T. F., Wojtczyk, H., Tenner, W. & Buzug, T. M. (2011, October). 1D-image reconstruction for magnetic particle imaging using a hybrid system function. *In Nuclear Science Symposium and Medical Imaging Conference (NSS/MIC)*, pp. 2545-2548.
- Hathaway, H., Butler, K., Adolphi, N., Lovato, D., Belfon, R., Fegan, D., Monson, T., Trujillo, J., Tessier, T., Bryant, H., Huber, D., Larson, R. and Flynn, E. (2011). Detection of breast cancer cells using targeted magnetic nanoparticles and ultra-sensitive magnetic field sensors. *Breast Cancer Research*, 13(5), pp. 1-13.
- Haro, L. P., Karaulanov, T., Vreeland, E. C., Anderson, B., Hathaway, H. J., Huber, D. L. & Flynn, E. R. (2015). Magnetic relaxometry as applied to sensitive cancer detection and localization. *Biomedical Engineering/Biomedizinische Technik*, 60(5), pp. 445-455.
- Harsanyi, B. B., Straub, M., & Schulz, V. (2015, March). An optimized receive-chain for MPI. *5th International Workshop on Magnetic Particle Imaging (IWMPI)*, pp. 1-1.
- Hennig, J., Welz, A., Schultz, G., Korvink, J., Liu, Z., Speck, O. & Zaitsev, M. (2008). Parallel imaging in non-bijective, curvilinear magnetic field gradients: a concept study. *Magnetic Resonance Materials in Physics, Biology, and Medicine*, 21(2), pp. 5-14.
- Hervault, A. & Thanh, N. T. K. (2014). Magnetic nanoparticle-based therapeutic agents for thermo-chemotherapy treatment of cancer. *Nanoscale*, 6(20), pp. 11553-11573.
- Horie, M., Tripathi, A., Ito, A., Kawabe, Y. & Kamihira, M. (2017). Magnetic Nanoparticles: Functionalization and Manufacturing of Pluripotent Stem Cells. *In Advances in Biomaterials for Biomedical Applications*, pp. 363-383.
- Huang, H. S. & Hainfeld, J. F. (2013). Intravenous magnetic nanoparticle cancer hyperthermia. *International Journal of Nanomedicine*, 8 (2013), pp. 2521-2532.

- Indira, T. K. & Lakshmi, P. K. (2010). Magnetic nanoparticles—a review. *International Journal of Pharmaceutical Sciences and Nanotechnology*, 3(3), pp. 1035-1042.
- Ishida, H. & Araki, K. (2004). Design and analysis of UWB Bandpass filter with ring filter. *In IEEE MTT-S International Microwave Symposium Digest*, 3, pp. 1307-1310.
- Ishihara, Y., Honma, T., Nohara, S. & Ito, Y. (2013). Evaluation of magnetic nanoparticle samples made from biocompatible ferucarbotran by time-correlation magnetic particle imaging reconstruction method. *BMC Medical Imaging*, 13(1), pp. 15.
- Isikman, S. O., Bishara, W., Sikora, U., Yaglidere, O., Yeah, J. & Ozcan, A. (2011). Field-portable lens free tomographic microscope. *Lab on a Chip*, 11(13), pp. 2222-2230.
- Issa, B., Obaidat, I. M., Albiss, B. & Haik, Y. (2013). Magnetic nanoparticles: surface effects and properties related to biomedicine applications. *International journal of molecular sciences*, 14(11), pp. 21266–21305.
- Johnson C., Adolphi N. L., Butler K. L., Lavato D. M., Larson R., Schwindt P. & Flynn E. R. (2012). Magnetic relaxometry with an atomic magnetometer and SQUID sensors on targeted cancer cells. *Journal of Magnetism and Magnetic Materials*. 24(1), pp. 2613–2619.
- Kaethner, C., Ahlborg, M., Gräfe, K., Bringout, G., Sattel, T. F. & Buzug, T. M. (2015). Asymmetric scanner design for interventional scenarios in magnetic particle imaging. *IEEE Transactions on Magnetics*, 51(2), pp. 1-4.
- Kala, S., Nalesh, S., Jose, B. R. & Mathew, J. (2018). Image Reconstruction Using Novel Two-Dimensional Fourier Transform. *In Advances in Soft Computing and Machine Learning in Image Processing*, pp. 699-718.
- Kang, T., Li, F., Baik, S., Shao, W., Ling, D. & Hyeon, T. (2017). Surface design of magnetic nanoparticles for stimuli-responsive cancer imaging and therapy. *Biomaterials*, 136, pp. 98-114.
- Karimi, M., Zare, H., Bakhshian Nik, A., Yazdani, N., Hamrang, M., Mohamed, E. & Hamblin, M. R. (2016). Nanotechnology in diagnosis and treatment of coronary artery disease. *Nanomedicine*, 11(5), pp. 513-530.
- Kaul, M. G., Mummert, T., Jung, C., Salamon, J., Khandhar, A. P., Ferguson, R. M. & Knopp, T. (2017). *In vitro* and *in vivo* comparison of a tailored magnetic

- particle imaging blood pool tracer with Resovist. *Physics in medicine and biology*, 62(9), pp. 3454.
- Khandhar, A. P., Ferguson, R. M., Arami, H. & Krishnan, K. M. (2013). Monodisperse magnetite nanoparticle tracers for in vivo magnetic particle imaging. *Biomaterials*, 34(15), pp. 3837-3845.
- Kilian, T., Fidler, F., Kasten, A., Nietzer, S., Landgraf, V., Weiß, K. & Steinke, M. (2016). Stem cell labeling with iron oxide nanoparticles: impact of 3D culture on cell labeling maintenance. *Nanomedicine*, 11(15), pp. 1957-1970.
- Kluth, T. & Maass, P. (2017). Model uncertainty in magnetic particle imaging: Motivating nonlinear problems by model-based sparse reconstruction. *International Journal on Magnetic Particle Imaging*, 3(2).
- Knopp, T. & Buzug, T. M. (2012). *Magnetic particle imaging: an introduction to imaging principles and scanner instrumentation*. Berlin: Springer Science & Business Media.
- Knopp, T. & Hofmann, M. (2016). Online reconstruction of 3D magnetic particle imaging data. *Physics in medicine and biology*, 61(11), N257.
- Knopp, T. & Weber, A. (2013). Sparse reconstruction of the magnetic particle imaging system matrix. *IEEE transactions on medical imaging*, 32(8), pp. 1473-1480.
- Knopp, T., Biederer, S., Sattel, T. F., Rahmer, J., Weizenecker, J., Gleich, B. & Buzug, T. M. (2010c). 2D model-based reconstruction for magnetic particle imaging. *Medical Physics*, 37(2), pp. 485-491.
- Knopp, T., Biederer, S., Sattel, T., Weizenecker, J., Gleich, B., Borgert, J. & Buzug, T. (2009). Trajectory analysis for magnetic particle imaging. *Physics in medicine and biology*, 54(2), pp. 385.
- Knopp, T., Erbe, M., Biederer, S., Sattel, T. F. & Buzug, T. M. (2010) Efficient generation of a magnetic field-free line. *Medical physics*, 37(1), pp. 3538.
- Knopp, T., Rahmer, J., Sattel, T. F., Biederer, S., Weizenecker, J., Gleich, B. & Buzug, T. M. (2010b). Weighted iterative reconstruction for magnetic particle imaging. *Physics in Medicine and Biology*, 55(6), pp. 1577.
- Knopp, T., Sattel, T. F., Biederer, S., Rahmer, J., Weizenecker, J., Gleich, B. & Buzug, T. M. (2011). Model-based reconstruction for magnetic particle imaging. *IEEE Transactions on Medical Imaging*, 29, pp. 12-18.

- Konkle, J. J., Goodwill, P. W., Hensley, D. W., Orendorff, R. D., Lustig, M. & Conolly, S. M. (2015). A convex formulation for magnetic particle imaging x-space reconstruction. *PloS one*, 10(10), e0140137.
- Konkle, J., Goodwill, P., Carrasco-Zevallos, O. & Conolly, S. (2013). Projection reconstruction magnetic particle imaging. *IEEE Transactions on Medical Imaging*, 32(2), pp. 338–347
- Kosch, O., Heinen, U., Trahms, L. & Wiekhorst, F. (2017). Preparing system functions for quantitative MPI. *International Journal on Magnetic Particle Imaging*, 3(2).
- Kötitz, R., Weitschies, W., Trahms, L. & Semmler, W. (1999). Investigation of Brownian and Neel relaxation in magnetic fluids. *Journal of magnetism and magnetic materials*, 201(1), 102-104.
- Kuehn, T., Bauerfeind, I., Fehm, T., Fleige, B., Hausschild, M., Helms, G. & Schmatloch, S. (2013). Sentinel-lymph-node biopsy in patients with breast cancer before and after neoadjuvant chemotherapy (SENTINA): a prospective, multicentre cohort study. *The lancet oncology*, 14(7), pp. 609-618.
- Kuo, J. & Shih, E. (2002). Wideband Bandpass filter design with three-line microstrip structures. *IEEE Proceedings on Microwaves, Antennas and Propagation*, 149, pp. 243-247.
- Le, T. A., Zhang, X., Hoshidar, A. K. & Yoon, J. (2017). Real-time two-dimensional magnetic particle imaging for electromagnetic navigation in targeted drug delivery. *Sensors*, 17(9), pp. 2050.
- Lee, Y. H., Kwon, H. C., Kim, J. M., Park, Y. K. & Park, J. C. (1997). A compact planar gradiometer system for measuring tangential components of biomagnetic fields. *IEEE transactions on applied superconductivity*, 7, pp. 2752-2755.
- Liu, H., Zhang, J., Chen, X., Du, X. S., Zhang, J. L., Liu, G. & Zhang, W. G. (2016). Application of iron oxide nanoparticles in glioma imaging and therapy: from bench to bedside. *Nanoscale*, 8(15), pp. 7808-7826.
- Lutovac, M. D., Tošić, D. V. & Evans, B. L. (2001). *Filter design for signal processing using MATLAB and Mathematica*. Upper Saddle River, New Jersey: Prentice Hall.
- Magnetic Insight. (2018). *About MPI: Magnetic Insight*. [Online] Available at: <https://www.magneticinsight.com/technology/> [Accessed 2 Jan. 2018].



- Markov, D. E., Boeve, H., Gleich, B., Borgert, J., Antonelli, A., Sfara, C. & Magnani, M. (2010). Human erythrocytes as nanoparticle carriers for magnetic particle imaging. *Physics in medicine and biology*, 55(21), pp. 6461.
- März, T. & Weinmann, A. (2016). Model-Based Reconstruction for Magnetic Particle Imaging in 2D and 3D. *arXiv preprint arXiv:1605.08095*.
- Maxwell, A. (2016). *Low-Frequency Electromagnetic Field Simulation*. Retrieved from <https://www.ansys.com/products/electronics/ansys-maxwell>.
- Miller, A. D. (2013). Lipid-based nanoparticles in cancer diagnosis and therapy. *Journal of drug delivery*, 10(9), pp. 1–9.
- Mizoguchi, T., Kandori, A., Kawabata, R., Ogata, K., Hato, T., Tsukamoto, A. & Enpuku, K. (2016). Highly sensitive third-harmonic detection method of magnetic nanoparticles using an AC susceptibility measurement system for liquid-phase assay. *IEEE Transactions on Applied Superconductivity*, 26(5), pp. 1-4.
- Mody, V. V., Cox, A., Shah, S., Singh, A., Bevins, W. & Parihar, H. (2014). Magnetic nanoparticle drug delivery systems for targeting tumor. *Applied Nanoscience*, 4(4), pp. 385-392.
- Morishige, T., Mihaya, T., Bai S., Miyazaki, T., Yoshida, T., Matsuo, M. & Enpuku, K. (2014). Highly sensitive Magnetic Nanoparticle Imaging using Cooled-Cu/HTS-Superconductor Pickup coils. *IEEE Transaction on Applied Superconductivity*, 24 (4). pp 105-109
- Murase, K. (2016). A simulation study on image reconstruction in magnetic particle imaging with field-free-line encoding. *arXiv preprint arXiv:1606.03188*.
- Murase, K., Hiratsuka, S., Song, R. & Takeuchi, Y. (2014). Development of a system for magnetic particle imaging using neodymium magnets and gradiometer. *Japanese Journal of Applied Physics*, 53(6), pp. 067001-067007.
- Muslu, Y., Utkur, M., Demirel, O. B. & Saritas, E. U. (2017). Calibration-Free Relaxation-Based Multi-Color Magnetic Particle Imaging. *arXiv preprint arXiv:1705.07624*.
- Natarajan, D. (2013). *Introduction to RF Filters: In A Practical Design of Lumped, Semi-lumped & Microwave Cavity Filters*. Heidelberg: Springer.
- Natividad, E. & Andreu, I. (2017). Characterization of Magnetic Hyperthermia in Magnetic Nanoparticles. *In Magnetic Characterization Techniques for Nanomaterials*, pp. 261-303.

- Nelson, R. C., Feuerlein, S. & Boll, D. T. (2011). New iterative reconstruction techniques for cardiovascular computed tomography: how do they work, and what are the advantages and disadvantages? *Journal of cardiovascular computed tomography*, 5(5), pp. 286-292.
- Novak, P., Shevchuk, A., Ruenraroengsak, P., Miragoli, M., Thorley, A. J., Klenerman, D. & Korchev, Y. E. (2014). Imaging single nanoparticle interactions with human lung cells using fast ion conductance microscopy. *Nano letters*, 14(3), pp. 1202-1207.
- Okubanjo, A. & Oyetola, K. (2012). *Design, construction, and simulation of third order Butterworth high-pass filter using MATLAB*. Retrieved from <https://www.researchgate.net>.
- Othman, N. B. (2014). *Magnetic Nanoparticle Imaging for Biomedical Applications*. (Doctoral thesis). Kyushu University, Fukuoka, Japan.
- Othman, N. B., Tsubaki, T., Yoshida, T., Enpuku, K. & Kandori, A. (2012). Magnetic Nanoparticle Imaging Using Harmonic Signals. *IEEE Transaction on Magnetics*, 48(11), pp. 3776-3779.
- Pablico-Lansigan, M. H., Situ, S. F. & Samia, A. C. S. (2013). Magnetic particle imaging: advancements and perspectives for real-time in vivo monitoring and image-guided therapy. *Nanoscale*, 5(10), pp. 4040-4055.
- Panagiotopoulos, N., Duschka, R. L., Ahlborg, M., Bringout, G., Debbeler, C., Graeser, M. & Buzug, T. M. (2015). Magnetic particle imaging: current developments and future directions. *International journal of nanomedicine*, 15(10), pp. 3097-3114.
- Pantic, I. (2010). Magnetic nanoparticles in cancer diagnosis and treatment: novel approaches. *Reviews on Advanced Materials Science e-Journal*, 26(1/2), pp. 67-73.
- Podaru, G.V., Chikan, V. & Prakash, P. (2016). Magnetic Field Induced Ultrasound from Colloidal Superparamagnetic Nanoparticles. *The Journal of Physical Chemistry C*, 120(4), pp. 2386-2391.
- Rahmer, J., Halkola, A., Gleich, B., Schmale, I. & Borgert, J. (2015). First experimental evidence of the feasibility of multi-color magnetic particle imaging. *Physics in medicine and biology*, 60(5), pp. 1775.

- Rahmer, J., Weizenecker, J., Gleich, B. & Borgert, J. (2009). Signal encoding in magnetic particle imaging: properties of the system function. *BMC medical imaging*, 9(1), 4, pp. 1-21.
- Rodolfo M., Antonio L., Liang C., Silvia G., Maria A. M., Francesco M., Marina S. & Francesco M. (2017, August 22). *Sentinel lymph node*. Retrieved from <http://www.tenderness.co/sentinel-lymph-node>.
- Rogge, H. & Schneider, R. (2011). Magnetic particle imaging (Doctoral thesis). Mathematisch-Naturwissenschaftliche Fakultät, Ernst-Moritz-Arndt-Universität, Greifswald, Germany.
- Roy, A. & Devoret, M. (2016). Introduction to parametric amplification of quantum signals with Josephson circuits. *Comptes Rendus Physique*, 17(7), pp. 740-755.
- Ruiz-Hernández, E., López-Noriega, A., Arcos, D., & Vallet-Regí, M. (2008). Mesoporous magnetic microspheres for drug targeting. *Solid State Sciences*, 10(4), pp. 421-426.
- Sadiq, A. A., Othman, N. B. & Jamil, M. M. A. (2016, December). Excitation coil design for single-sided magnetic particle imaging scanner. *In IEEE Asia-Pacific Conference on Applied Electromagnetics*, pp. 364-368.
- Sadiq, A. A., Othman, N. B. & Mahadi, A. M. (2015). Magnetic particle imaging system for cancer diagnosis: an overview. *ARPJ Journal of Engineering and Applied Sciences*, 10 (19), pp. 8556-8561.
- Sanvicens, N. & Pilar Marco, M. (2008). Multifunctional nanoparticles- properties and prospects for their use in human medicine. *Bioengineering and Biomaterials*, 4 (5), pp. 425-433.
- Saritas, E. U., Goodwill, P. W., Croft, L. R., Konkle, J. J., Lu, K., Zheng, B. & Conolly, S. M. (2013). Magnetic particle imaging (MPI) for NMR and MRI researchers. *Journal of Magnetic Resonance*, 229, pp. 116-126.
- Saritas, E. U., Goodwill, P. W., Zhang, G. Z. & Conolly, S. M. (2013). Magnetostimulation limits in magnetic particle imaging. *IEEE transactions on medical imaging*, 32(9), pp. 1600-1610.
- Sasayama, T., Tsujita, Y., Morishita, M., Muta, M., Yoshida, T. & Enpuku, K. (2017). Three-dimensional magnetic nanoparticle imaging using small field gradient and multiple pickup coils. *Journal of Magnetism and Magnetic Materials*, 427, pp. 143-149.

- Sattel, F. T., Knopp, T., Biederer, S., Gleich, B., Weizenecker, J., Borgert, J. & Buzug, T. (2009). Single-sided device for magnetic particle imaging. *Journal of applied physics*, 42(2), pp. 1-5.
- Schmidt, D., Eberbeck, D., Steinhoff, U. & Wiekhorst, F. (2017). Finding the magnetic size distribution of magnetic nanoparticles from magnetisation measurements via the iterative kaczmarz algorithm. *Journal of Magnetism and Magnetic Materials*, 431, pp. 33-37.
- Schneider, M. G. M. & Lassalle, V. L. (2017). Magnetic iron oxide nanoparticles as novel and efficient tools for atherosclerosis diagnosis. *Biomedicine & Pharmacotherapy*, 93, pp. 1098-1115.
- Schulz, V., Straub, M., Mahlke, M., Hubertus, S., Lammers, T. & Kiessling, F. (2015). A field cancellation signal extraction method for magnetic particle imaging. *IEEE transactions on magnetics*, 51(2), pp. 1-4.
- Sebastián, J., Fernández-Miaja, P., Rodríguez, A. & Rodríguez, M. (2014). Analysis and design of the output filter for buck envelope amplifiers. *IEEE Transactions on Power Electronics*, 29(1), pp. 213-233.
- Seton, H. C., Hutchison, J. M. S. & Bussell, D. M. (1999). Gradiometer pick-up coil design for a low field SQUID-MRI system. *Magnetic Resonance Materials in Physics, Biology and Medicine*, 8(2), pp. 116-120.
- Shah, S. A., Reeves, D. B., Ferguson, R. M., Weaver, J. B. & Krishnan, K. M. (2015). Mixed Brownian alignment and Néel rotations in superparamagnetic iron oxide nanoparticle suspensions driven by an AC field. *Physical Review B*, 92(9), pp. 094438.
- Shen, W. B., Anastasiadis, P., Nguyen, B., Yarnell, D., Yarowsky, P. J., Frenkel, V. & Fishman, P. S. (2017). Magnetic Enhancement of Stem Cell-Targeted Delivery into the Brain Following MR-Guided Focused Ultrasound for Opening the Blood-Brain Barrier. *Cell Transplantation*, 26(7), pp. 1235-1246.
- Silva, S. R., Battarai, K., Shields, A. & Zhou, J. (2017). Enhanced Second-harmonic Generation Using Nonlinear Metamaterials. *arXiv preprint arXiv:1705.07720*.
- Simsek, E. & Kilic, M. A. (2005). Magic ferritin: A novel chemotherapeutic encapsulation bullet. *Journal of magnetism and magnetic materials*, 293(1), pp. 509-513.
- Singh, A. & Sahoo, S. K. (2014). Magnetic nanoparticles: a novel platform for cancer theranostics. *Drug Discovery Today*, 19(4), pp. 474-481.

- Song, K. H., Kim, C., Cobley, C. M., Xia, Y. & Wang, L. V. (2008). Near-infrared gold nanocages as a new class of tracers for photoacoustic sentinel lymph node mapping on a rat model. *Nano letters*, 9(1), pp. 183-188.
- Sosnovick, D. E., Nahrendorf, M. & Weissleder, R. (2008). Magnetic nanoparticle for MR imaging: agents, techniques and cardiovascular applications. *Basic Research in Cardiology*, 103 (2), pp 122-130.
- Spencer, M. P. & Yamamoto, N. (2016). Nanoparticle Alignment using Oscillating Magnetic Fields for Scalable Nanocomposite Manufacturing. In *57th AIAA/ASCE/AHS/ASC Structures, Structural Dynamics, and Materials Conference*, pp. 0150.
- Suetens, P. (2017). *Fundamentals of medical imaging*. Cambridge university press.
- Tanaka, S., Murata, H., Oishi, T., Hatsukade, Y., Zhang, Y., Horng, H. E. & Yang, H. C. (2015). Imaging of magnetic nanoparticles using a second harmonic of magnetisation with DC bias field. *IEEE Transactions on Magnetics*, 51(2), pp. 1-4.
- Tanaka, S., Murata, H., Oishi, T., Suzuki, T. & Zhang, Y. (2014). 2D magnetic nanoparticle imaging using Magnetisation response second harmonic. *Journal of Magnetism and Magnetic Materials*, 1(5), pp. 1-16.
- Tanaka, S., Suzuki, T., Kobayashi, K., Liao, S. H., Horng, H. E. & Yang, H. C. (2017). Analysis of magnetic nanoparticles using second harmonic responses. *Journal of Magnetism and Magnetic Materials*, 440, pp. 189-191.
- Thong, W. M. & Gunstone, R. (2008). Some student conceptions of electromagnetic induction. *Research in Science Education*, 38(1), pp. 31-44.
- Trakic, A., Liu, L., Lopez, H. S., Zilberti, L., Liu, F. & Crozier, S. (2014). Numerical safety study of currents induced in the patient during rotations in the static field produced by a hybrid MRI-LINAC system. *IEEE Transactions on Biomedical Engineering*, 61(3), pp. 784-793.
- Tsuchiya, H., Shimizu, S., Hatsuda, T., Takagi, T., Noguchi, T. & Ishihara, Y. (2015, March). Two-dimensional magnetic imaging system for evaluating iterative reconstruction method based on time-correlation information. In *(IWMPI), 2015 5th International Workshop on Magnetic Particle Imaging*, pp. 1-1.
- Tumanski, S. (2007). Induction coil sensors—A review. *Measurement Science and Technology*, 18(3), pp. R31-R46.

- Tumanski, S. (2016). *Handbook of magnetic measurements*. Boca Raton, Florida: CRC Press.
- Uchida S., Higuchi, Y., Ueoka, Y., Yoshida, T., Enpuku, K., Adachi, S., Tanabe, K., Tsukamoto, A. & Kandori, A. (2014). Highly sensitive liquid-phase detection of biological targets with magnetic markers and high T<sub>c</sub> SQUID. *IEEE Transactions on Applied Superconductivity*, 24, pp. 1600105.
- Utkur, M., Muslu, Y. & Saritas, E. U. (2017). Relaxation-based viscosity mapping for magnetic particle imaging. *Physics in Medicine and Biology*, 62(9), pp. 3422.
- Vaalma, S., Rahmer, J., Panagiotopoulos, N., Duschka, R. L., Borgert, J., Barkhausen, J. & Haegele, J. (2017). Magnetic Particle Imaging (MPI): Experimental Quantification of Vascular Stenosis Using Stationary Stenosis Phantoms. *PLoS one*, 12(1), pp. e0168902.
- Vrba, J., Haid, G. J., Lee, W. M. S., Taylor, B. R. & Tillotson, M. A. (2007). U.S. Patent No. 5,657,756. Washington, DC: U.S. Patent and Trademark Office.
- Waanders, S., Visscher, M., Wildeboer, R. R., Oderkerk, T. O. B., Krooshoop, H. J. & ten Haken, B. (2016). A handheld SPIO-based sentinel lymph node mapping device using differential magnetometry. *Physics in medicine and biology*, 61(22), pp. 8120-8134.
- Wadajkar, A. S., Menon, J. U., Kadapure, T., Tran, R. T. & Yang, J. (2013). Design and application of magnetic-based theranostic nanoparticle systems. *Recent patents on biomedical engineering*, 6(1), pp. 47-57.
- Wang, J. Y., Healey, T., Barker, A., Brown, B., Monk, C. & Anumba, D. (2017). Magnetic induction spectroscopy (MIS)-probe design for cervical tissue measurements. *Physiological Measurement*, 38(5), pp. 729.
- Wang, X., Shellock, F. & Shellock Frank G. (2014). Markers for visualizing interventional medical devices. U.S. Patent Application, 10(999), pp. 185.
- Weber, A., Weizenecker, J., Heinen, U., Heidenreich, M. & Buzug, T. M. (2015). Reconstruction enhancement by denoising the magnetic particle imaging system matrix using frequency domain filter. *IEEE Transactions on Magnetics*, 51(2), pp. 1-5.
- Weizenecker, J., Borgert, J. & Gleich, B. (2007). A simulation study on the resolution and sensitivity of magnetic particle imaging. *Physics in Medicine and biology*, 52(21), pp. 6363.

- Weizenecker, J., Gleich, B. & Borgert, J. (2008). Magnetic particle imaging using a field free line. *Journal of Physics D: Applied Physics*, 41(10), 105009.
- Weizenecker, J., Gleich, B., Rahmer, J., Dahnke, H. & Borgert, J. (2009). Three-dimensional real-time in vivo magnetic particle imaging. *Physics in medicine and biology*, 54(5), L1.
- Winder, S. (2002). *Analog and digital filter design*. Oxford: Newnes.
- Woods, R. C., Baker, R. M., Li, F., Stephenson, G. V., Davis, E. W. & Beckwith, A. W. (2011). A new theoretical technique for the measurement of high-frequency relic gravitational waves. *Journal of Modern Physics*, 2(06), pp. 498.
- Wu, G., Wang, B., Yuan, Y., Zhang, C. & Tian, G. (2017). A fast interpretation method of gravity gradiometry data based on magnetic dipole localization. *Journal of Applied Geophysics*, 141, 47-53.
- Wu, K., Batra, A., Jain, S. & Wang, J. P. (2016). Magnetisation Response Spectroscopy of Superparamagnetic Nanoparticles under Mixing Frequency Fields. *IEEE Transactions on Magnetics*, 52(7), pp. 1-4.
- Wu, K., Wang, Y., Feng, Y., Yu, L. & Wang, J. P. (2015). Colorize magnetic nanoparticles using a search coil based testing method. *Journal of Magnetism and Magnetic Materials*, 380, pp. 251-254.
- Yan, H., Guo, M. & Liu, K. (2006). Multifunctional Magnetic Hybrid Nanoparticles as a Nanomedical Platform for Cancer-Targeted Imaging and Therapy. *In Biomedical Science, Engineering and Technology*, 2(11), pp. 283-300.
- Yang, C. C., Yang, S. Y., Chen, H. H., Weng, W. L., Horng, H. E., Chieh, J. J., Hong, C. Y. & Yang, H. C. (2012). Effect of molecule-particle binding on the reduction in the mixedfrequency alternating current magnetic susceptibility of magnetic bio-reagents. *Journal of Applied Physics*, 112, pp. 024704.
- Yao, L. & Xu, S. (2014). Detection of magnetic nanomaterials in molecular imaging and diagnosis applications. *Nanotechnology Reviews*, 3(3), pp. 247-268.
- Yoshida, T., Othman, N. B., Tsubaki, T., Ogawa, K. & Enpuku, K. (2011). Detection of Magnetic Nanoparticles using the Second-Harmonic Signal. *IEEE Transaction on Magnetics*, 47 (10), pp 2863-2866.
- Yoshida, T., Othman, N. B., Tsubaki, T., Takamiya, J. & Enpuku, K. (2012). Evaluation of Harmonic Signals for the detection of magnetic Nanoparticles. *IEEE Transaction on Magnetics*, 48 (11), pp. 3788-3791.

- Yu, E. Y., Bishop, M., Zheng, B., Ferguson, R. M., Khandhar, A. P., Kemp, S. J. & Conolly, S. M. (2017). Magnetic particle imaging: a novel in vivo imaging platform for cancer detection. *Nano Letters*, 17(3), pp. 1648-1654.
- Yu, M. K., Park, J. & Jon, S. (2012). Targeting strategies for multifunctional nanoparticles in cancer imaging and therapy. *Theranostics*, 2(1), pp. 3–44.
- Zehra, A. (2014). Design and simulation of 4th order active Bandpass filter using multiple feedback and Sallen key topologies. *Journal of Babylon University*, 2, pp. 463-473.
- Zhang, Y., Murata, H., Hatsukade, Y. & Tanaka, S. (2013). Superparamagnetic nanoparticle detection using second harmonic of magnetisation response. *Review of scientific instruments*, 84(9), pp. 094702.
- Zhao, Z., Torres-Díaz, I., Vélez, C., Arnold, D. & Rinaldi, C. (2016). Brownian Dynamics Simulations of Magnetic Nanoparticles Captured in Strong Magnetic Field Gradients. *The Journal of Physical Chemistry C*, 121(1), pp. 801-810.
- Zheng, B., Vazin, T., Goodwill, P. W., Conway, A., Verma, A., Saritas, E. U. & Conolly, S. M. (2015). Magnetic particle imaging tracks the long-term fate of in vivo neural cell implants with high image contrast. *Scientific reports*, 5, pp. 112-119.
- Zhou, X. Y., Jeffris, K. E., Elaine, Y. Y., Zheng, B., Goodwill, P. W., Nahid, P. & Conolly, S. M. (2017). First in vivo magnetic particle imaging of lung perfusion in rats. *Physics in Medicine and Biology*, 62(9), pp. 3510-3522.

